M&C 2017 - International Conference on Mathematics & Computational Methods Applied to Nuclear Science & Engineering, Jeju, Korea, April 16-20, 2017, on USB (2017)

Comparison of 1D Green's Functions in the PN and BN Approximations of Monoenergetic Neutron Transport Theory

G. Giudicelli, C. Josey, J. Miao and B. Ganapol
Department of Nuclear Science and Engineering, MIT
Cambridge, MA
and
S. Woolf
ARCON CORP, Waltham, MA

Abstract – *An investigation of the infinite Green's function scalar flux in the BN and PN approximations for isotropic source emission for monoenergetic neutron transport is presented. The approximations are clearly defined by closure of the Legendre moments. The formulation features full scattering anisotropy. A numerical Fourier transform inversion then shows the two approximations give nearly identical results to 7-places beyond 1mfp from the source.*

I. INTRODUCTION

The Green's function is fundamental to all solutions of the linear neutron transport equation. It represents an analytical foundation upon which a transport solution is rooted and leads to analytical simplification of solutions in finite media. In this presentation, we consider the monoenergetic Green's function in 1D-- specifically for an isotropically emitting source but featuring general anisotropic scattering in both the PN and BN approximations. Our presentation derives the PN and BN approximations through closure of the transport equation enabling analytical solution representations in terms of Fourier transform inversions. For the BN approximation, we then, numerically evaluate its Fourier transform and perform a numerical inversion coupling Talbot's contour to convergence acceleration in the approximation order *N*. An analytical inversion gives the PN approximation. From convergence acceleration in *N*, one achieves highly precise scalar fluxes in both cases. In addition, we compare the PN and BN scalar fluxes to an MCNPX Monte Carlo simulation.

The objectives of this work are threefold. Our first objective is to demonstrate how the analytical solution to the neutron transport equation in Fourier transform space for general anisotropic scattering leads to a precise numerical inversion through convergence acceleration. The second objective is to introduce an improved numerical Fourier transform inversion based on Talbot's algorithm. Finally, the last objective is to observe the difference between the two approximations and with Monte Carlo.

This presentation should appeal to those involved in development of analytical methods in transport theory and analytical methods in general. In addition, those concerned with how one monitors numerical methods to give high precision from seemingly ordinary numerical methods should be interested. Finally, researchers interested in PN and/or BN theory may also appreciate our approach.

II. PN/BN THEORIES

The 1D Green's function comes from the solution to the following neutron transport equation:

$$\left[\mu\frac{\partial}{\partial x}+1\right]\psi\left(x,\mu;\mu_0\right)= \tag{1a}$$
$$=\frac{c}{2}\sum_{l=0}^{\infty}\omega_l P_l\left(\mu\right)\psi_l\left(x;\mu_0\right)+\delta\left(\mu-\mu_0\right)\delta\left(x\right),$$

where c is the ratio of scattering to total cross section, x is measured in units of mean free path and the scattering phase function is represented in the Legendre polynomial basis. In addition,

$$\lim_{|x|\to\infty}\psi\left(x,\mu;\mu_0\right)<\infty, \tag{1b}$$

$$\sum_{l=0}^{\infty}\left|\omega_l\right|<\infty \tag{1c}$$

to keep the scattering integral convergent.

In the usual way, taking the Fourier transform

$$\bar{\psi}\left(k,\mu;\mu_0\right)\equiv\int_{-\infty}^{\infty}dxe^{-ikx}\psi\left(x,\mu;\mu_0\right)$$

and solving for the transformed moments

$$\bar{\psi}_l\left(k;\mu_0\right)\equiv\int_{-\infty}^{\infty}dxe^{-ikx}\psi_l\left(x;\mu_0\right)$$

gives [1]

$$\sum_{l=0}^{\infty}\left[\delta_{j,l}-c\omega_l L_{j,l}\left(z\right)\right]\bar{\psi}_l\left(k;\mu_0\right)=\frac{z}{z-\mu_0}P_j\left(\mu_0\right) \tag{2a}$$

with

$$L_{j,l}\left(z\right)\equiv z\begin{cases}Q_l\left(z\right)P_j\left(z\right), & j\le l\\ Q_j\left(z\right)P_l\left(z\right), & l<j\end{cases} \tag{2b}$$

and $z \equiv -1/ik$. Note that P_l and Q_l are respectively Legendre polynomials and functions of the second kind.

One can show the transformed moments satisfy the recurrence

$$zh_l\bar{\psi}_l(k;\mu_0) - (l+1)\bar{\psi}_{l+1}(k;\mu_0) - l\bar{\psi}_{l-1}(k;\mu_0) = = zS_l(\mu_0) \quad (3a)$$

with

$$h_l \equiv 2l + 1 - c\omega_l$$
$$S_l(\mu_0) \equiv (2l+1)P_l(\mu_0) \quad (3b,c)$$

yielding (after some algebra) the analytical solution [1]

$$\bar{\psi}_l(k;\mu_0) = g_l(z)\bar{\psi}_0(k;\mu_0) + \sum_{j=0}^{l}(2j+1)\left[\rho_j(z)g_l(z) - g_j(z)\rho_l(z)\right]P_j(\mu_0) \quad (3d)$$

In this representation, the Chandrasekhar polynomials of the first and second kinds satisfy

$$g_0(z) = 1$$
$$zh_l g_l(z) - (l+1)g_{l+1}(z) - lg_{l-1}(z) = 0, \quad (3e,f)$$

and

$$\rho_0(z) = 0$$
$$zh_l\rho_l(z) - (l+1)\rho_{l+1}(z) - l\rho_{l-1}(z) = -z\delta_{l,0} \quad (3g,h)$$

respectively.

Significant simplification results when we are only interested in the Green's function for an isotropically emitting source found by integrating μ_0 over [-1.1] and normalizing to ½ to give the moments

$$\bar{\psi}_l(k) = \frac{1}{2}\int_{-1}^{1} d\mu_0 \bar{\psi}_l(k;\mu_0). \quad (4a)$$

Therefore, from Eq(3d),

$$\bar{\psi}_l(k) = g_l(z)\bar{\psi}_0(k) - \rho_l(z), \quad (4b)$$

and from Eq(2a)

$$\sum_{l=0}^{\infty}\left[\delta_{j,l} - c\omega_l L_{j,l}(z)\right]\bar{\psi}_l(k) = zQ_j(z) \quad (4c)$$

It is apparent that the scalar flux transform $\bar{\psi}_0(k)$ is yet to be specified. For this reason, we require an independent relation for closure, which will lead to the PN and BN approximations.

1. PN Closure

The first closure is the PN closure yielding PN theory. In particular, one assumes the N+1 and higher transformed moments in the Legendre expansion of the scalar flux to vanish. Hence,

$$\bar{\psi}_{l+1}(k) \equiv 0;\ l = N, ...; \quad (5a)$$

and immediately, from Eq(4b) with $l = N$, therefore,

$$\bar{\psi}_{0,N}^{PN}(k) = \frac{\rho_{N+1}(z)}{g_{N+1}(z)}. \quad (5b)$$

closes the system. Note the additional subscript to indicate closure at N.

2. BN Closure

Transport, or BN, closure results when one truncates the scattering representation

$$\omega_l = 0,\ l \geq N+1.$$

Now Eq(4c) for j = 0 with Eq(4b) introduced for the moments is solved for the zeroth moment to give

$$\bar{\psi}_{0,N}^{BN}(k) = \frac{\gamma_N(z)}{\Lambda_N(z)}, \quad (6a)$$

where, from the Christofel-Darboux (CD) formula [2],

$$\Lambda_N(z) = (N+1)\left[g_{N+1}(z)Q_N(z) - g_N(z)Q_{N+1}(z)\right]$$
$$\gamma_N(z) = (N+1)\left[\rho_{N+1}(z)Q_N(z) - \rho_N(z)Q_{N+1}(z)\right]. \quad (6b,c)$$

For example, to derive Eq(6b), one multiplies the recurrence for $Q_l(z)$,

$$z(2l+1)Q_l(z) - (l+1)Q_{l+1}(z) - lQ_{l-1}(z) = 0,$$

by $g_l(z)$ and the recurrence for $g_l(z)$, Eq(3e,f), by $Q_l(z)$, subtracts and sums over l. Similarly for Eq(6c) using the recurrence Eq(3g,h) for $\rho_l(z)$.

III. ANALYTICAL INVERSIONS

We are now in position to perform the Fourier transform inversion for the scalar flux

$$\psi_{0,N}(x) \equiv \frac{1}{2\pi}\int_{-\infty}^{\infty} dk e^{ikx}\bar{\psi}_{0,N}(k), \quad (7)$$

where the image function $\bar{\psi}_{0,N}(k)$ is either Eq(5b) or (6a).

1. For PN

From the N+1 poles of the PN approximation (roots of $g_{N+1}(z) = 0$), the analytical inversion can be shown to be

$$\psi_{0,N}^{PN}(x)=\sum_{j=1}^{(N+1)/2}\frac{e^{-x/z_j}}{z_j\sum_{k=0}^{N}h_k g_k(z_j)^2}. \tag{8}$$

A more numerically appropriate form adds and subtracts the uncollided contribution

$$\psi_{0,N}^{PN}(x)=\frac{1}{2}E_1(x)+$$
$$+\sum_{j=1}^{(N+1)/2}\left\{\frac{e^{-x/z_j}}{z_j\sum_{k=0}^{N}h_k g_k(z_j)^2}-\frac{e^{-x/\varsigma_j}}{\varsigma_j\sum_{k=0}^{N}(2k+1)P_k(\varsigma_j)^2}\right\}, \tag{9}$$

where the first term is the exponential integral and ς_j is the *j*th root of the *n*+1 Legendre polynomial.

2. For BN

The BN inversion is not as simple as the PN since the inversion

$$\psi_{0,N}^{BN}(x)\equiv\frac{1}{2\pi}\int_{-\infty}^{\infty}dk e^{ikx}\frac{\gamma_N(z)}{\Lambda_N(z)}. \tag{10}$$

includes poles and branch points of the dispersion relation $\Lambda_N(z)$.

Our choice of evaluation is exclusively numerical, where we analytically continue from the real line into the complex plane and deform the contour around the branch cut on the imaginary axis as shown in Fig. 1.

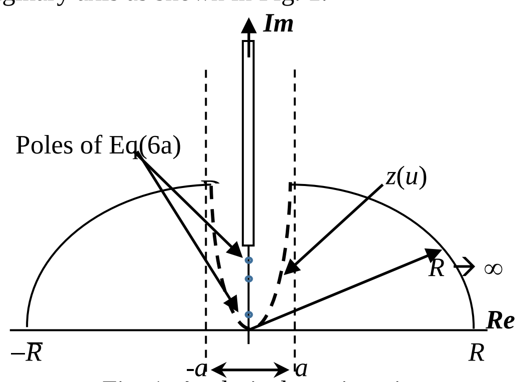

Fig. 1. Analytical continuation.

The Talbot contour [3], $z(u)$, shown in Fig. 1, is chosen as

$$z(u)=u\big(1+g(u)i\big),\quad -a\le u\le a$$
$$g(u)=\tan\left(\frac{\pi u}{2a}\right)\to\infty,\quad u\to\pm a \tag{11a,b}$$

The contour is constructed such that it tends to infinity at the ends of a finite interval [-*a*,*a*] as the circular arcs of radius *R* tend to infinity. The advantage is to take an improper integral with a highly oscillating integrand into one that can be evaluated over a finite interval. Intuitively, this seems like a numerical advantage. Of course, it depends on the variation of the integrand as a function of *u* in [-*a*,*a*]. The resulting integral using the specific analytical properties of *z*(-*u*) is

$$\psi_{0,N}^{BN}(x)\equiv$$
$$\equiv\frac{1}{\pi}\int_0^a du\, e^{-ug(u)x}Re\left\{\frac{dz(u)}{du}\left[\frac{\gamma_N(z(u))}{\Lambda_N(z(u))}\right]e^{iux}\right\}. \tag{12}$$

With this procedure, knowledge of the poles are not required, avoiding the difficulty for situations when *c* is near unity. The disadvantage is that we must evaluate the Chandrasekhar polynomials and Legendre functions for complex arguments rather than simply imaginary arguments on either side of the branch cut.

IV. NUMERICAL IMPLEMENTATION AND DEMONSTRATION

1. Implementation

Both inversions require the Chandrasekhar *g*-polynomial, which come from the following scaled recurrence of Eqs(3e,f):

$$z\hat{g}_l(z)-\omega_l\hat{g}_{l+1}(z)-\omega_{l-1}\hat{g}_{l-1}(z)=0 \tag{13a}$$

$$\omega_l\equiv(l+1)/\sqrt{h_l h_{l+1}} \tag{13b}$$

$$g_l(z)=\hat{g}_l(z)\sqrt{n_l},\ n_l\equiv 2/h_l. \tag{13c}$$

Note that here ω_l is not the same as the scattering coefficients.

Thus, in vector form Eq(13a) becomes

$$\left[\boldsymbol{A}_{1,l+1}(0)-z\boldsymbol{I}\right]\hat{\boldsymbol{g}}_l(z)=\omega_l\hat{g}_{l+1}(z)\begin{bmatrix}0 & \dots & 0 & 1\end{bmatrix}^T \tag{14a}$$

where

$$\boldsymbol{A}_{1,l+1}(0)\equiv\begin{bmatrix}0 & \omega_0 & 0 & \dots & & 0\\ \omega_0 & 0 & \omega_1 & 0 & \dots & 0\\ 0 & \omega_1 & 0 & \omega_2 & & \dots\\ \dots & & \dots & \dots & \dots & 0\\ 0 & & 0 & \omega_{l-2} & 0 & \omega_{l-1}\\ 0 & \dots & & 0 & \omega_{l-1} & 0\end{bmatrix} \tag{14b}$$

with

$$\hat{\boldsymbol{g}}_l(z) = \left[\hat{g}_0(z) \quad \dots \quad \hat{g}_{l-1}(z) \quad \hat{g}_l(z)\right]^T . \quad (14c)$$

The roots z_j required in Eq(9) are simply the eigenvalues of the matrix $\boldsymbol{A}_{1,N+1}(0)$. Chandrasekhar polynomials can therefore be expressed in terms of their roots

$$g_l(z) = (-1)^l \sqrt{\frac{h_0}{h_l}} \left[\prod_{j=0}^{l-1} \omega_j\right]^{-1} \prod_{j=1}^{l} \left(\lambda_{1Rlj} - z\right)$$
$$\rho_l(z) = (-1)^{l-1} z \sqrt{\frac{h_1}{h_l}} \left[\prod_{j=0}^{l-1} \omega_j\right]^{-1} \prod_{j=1}^{l-1} \left(\lambda_{2Rlj} - z\right) \quad (15a,b)$$

where λ_{1Rlj} and λ_{2Rlj} are the eigenvalues of $\boldsymbol{A}_{1,N}(0)$ and the eigenvalues of the corresponding matrix,

$$\boldsymbol{A}_{2,N}(0) \equiv \begin{bmatrix} 0 & \omega_1 & 0 & \dots & & 0 \\ \omega_1 & 0 & \omega_2 & 0 & \dots & 0 \\ 0 & \omega_2 & 0 & \omega_3 & & \dots \\ \dots & & \dots & \dots & \dots & 0 \\ 0 & & 0 & \omega_{l-3} & 0 & \omega_{N-2} \\ 0 & \dots & & 0 & \omega_{N-2} & 0 \end{bmatrix}.$$

for polynomials of the second kind.

Also required for the BN approximation is Q_l as determined by the usual recurrence for $|z|<1$

$$Q_0(z) = \frac{1}{2}\ln\left[\frac{z+1}{z-1}\right]$$
$$(2l+1) z Q_l(z) - (l+1) Q_{l+1}(z) - l Q_{l-1}(z) = -z\delta_{l,0} \quad (16a,b)$$

and for $|z|>1$ [4]

$$Q_l(z) = \sqrt{\pi}\frac{l!}{\Gamma(l+3/2)} w^{l+1} {}_2F_1\left(l+1, 1/2; l+3/2, w^2\right) \quad (16c)$$

with $w \equiv z - \sqrt{z^2-1}$ and ${}_2F_1$ is a hypergeometric function.

2. Demonstration

For our demonstration, we assume scattering from hydrogen whose monoenergetic anisotropic scattering expansion coefficients are

$$\omega_0 = 1, \ \omega_1 = 2$$
$$\omega_l \equiv 2(2l+1)\int_0^1 dss P_l(s); \ l = 2, \dots. \quad (17a)$$

giving for the even moments:

$$\xi_{m+1} = \frac{1}{2}\left[\frac{1-2m}{m+2}\right]\xi_m, \ \xi_0 = 1, \quad (17b)$$

where $\omega_{2m} = (2m+1)\xi_m$. The odd moments, after the first, vanish.

Table I gives a comparison of BN and PN approximations for an isotropic source at x = 0 out to 10 *mfp* from the source for c = 0.9. We apply Wynn-epsilon (*W-e*) convergence acceleration [5] in the approximation order N to both approximations. The BN approximation with *W-e* converged at order 29 to at least 11 places. Column 3 gives the maximum relative error between iterates when *W-e* converged over all tabulated spatial points. It is apparent that convergence without acceleration is most difficult near the source. Column 4, which is the ratio of the relative error between iterates of the unconverged to the converged when all spatial points have converged by *W-e*, confirms this observation. Clearly, *W-e* has a distinct advantage near the source.

The last two columns gives the PN converged flux and the order at convergence. Except near the source, PN is as precise as BN. Further investigation of the PN error needs to be performed however. In particular-- Is the error from the uncollided approximation, which is most important near the source?

Table I. Comparison of BN and PN

x	*BN Flux N= 29*	*Rel. Error*	*Error Ratio*	*PN Flux*	*Nmax*
0.01	3.5053587E+00	4.49E-12	2.185E+05	3.5053955E+00	320
1	1.1750734E+00	1.17E-11	7.285E+02	1.1750735E+00	86
2	7.9026022E-01	7.43E-12	1.052E+01	7.9026022E-01	74
3	5.5765719E-01	5.38E-11	1.017E+01	5.5765719E-01	46
4	3.9856021E-01	3.40E-13	8.576E-02	3.9856021E-01	38
5	2.8604237E-01	1.92E-14	2.416E-02	2.8604237E-01	34
6	2.0560008E-01	7.50E-14	9.444E-01	2.0560008E-01	30
7	1.4786649E-01	1.55E-13	4.132E-03	1.4786649E-01	26
8	1.0636983E-01	1.56E-14	8.000E-02	1.0636983E-01	26
9	7.6526132E-02	4.24E-14	5.263E-02	7.6526132E-02	22
10	5.5057842E-02	8.06E-15	3.806E-03	5.505784 E-02	22

As a final result, Table 2 gives infinite medium fluxes for variation of the number of histories as determined by MCNPX [6]. Apparently, a relatively large effort is required to obtain consistent 3-place agreement from MCNPX. Also note that the Monte Carlo calculation seems to be converging toward the benchmark.

V. CONCLUSION

In this work, we have the beginning of a comprehensive study of the monoenergetic BN and PN approximations in a 1D-plane infinite medium. The origin of the two approximations is clearly derived. With the help of convergence acceleration, we have found the two numerical approximations virtually indistinguishable after one *mfp* from the source. The analysis for the Green's function for an isotropic source presented here will form the basis for analysis of the full Green's function in a future effort.

Additional effort will be directed toward perfecting the numerical inversion as well as using the Green's function to provide benchmarks for heterogeneous media.

Table 2. MCNPX Infinite medium

x\# Histories	10^3	10^5	10^7	10^9
0.01	3.51321379E+00	3.47669867E+00	3.50276711E+00	3.50345665E+00
1	1.12800734E+00	1.16298512E+00	1.17384044E+00	1.17375658E+00
2	7.75056244E-01	7.89570097E-01	7.90453561E-01	7.90417587E-01
3	5.47176464E-01	5.57462498E-01	5.59179887E-01	5.59100051E-01
4	3.93944508E-01	3.96831678E-01	3.98871497E-01	3.98805846E-01
5	2.92786817E-01	2.86864580E-01	2.85915676E-01	2.85827900E-01
6	1.90243965E-01	2.07675190E-01	2.05394038E-01	2.05338196E-01
7	1.33889955E-01	1.46916972E-01	1.47985731E-01	1.47922640E-01
8	1.04852614E-01	1.05929308E-01	1.06433564E-01	1.06418733E-01
9	6.91816430E-02	7.55479900E-02	7.63436977E-02	7.63400246E-02
10	5.42119205E-02	5.44841046E-02	5.50902082E-02	5.51079203E-02

REFERENCES

1. B. Ganapol, The Infinite Medium Green's Function of Monoenergetic Neutron Transport Theory via Fourier Transform, *Nucl. Sci. & Eng.*, V180, Number 2, 224-246 (2015).
2. E. Inönü, Orthogonally of a set of polynomials encountered in neutron transport and radiative transfer theories, *J. Math. Phys.*, **11**, 568-577 (1970).
3. A. Talbot, The accurate numerical inversion of Laplace transforms. In: J. Inst. Math. Appl. 23 (1979), Nr. 1, S. 97–120. – ISSN 0020–2932 1, 2, 3, 9.

4 V.I. Lebedev, *Special Functons and Their Applications*, Prentice Hall, NJ, 1965.

5 A. Sidi, *Practical Extrapolations Methods*, Cambridge University Press, Cambridge, UK (2003).

6. RSICC COMPUTER CODE COLLECTION, MCNPX™ 2.4.0 USER MANUAL, ORNL.